

OPEN ACCESS

EDITED BY Evan Siemann, Rice University, United States

REVIEWED BY Zhili Pan, Yunnan University, China Yang Wenjun, Fudan University, China

RECEIVED 25 August 2025 ACCEPTED 21 October 2025 PUBLISHED 17 November 2025

CITATION

Fan Y, Zhang X, Yang J, Yang J, Zhang H, Yang B and Li X (2025) Prediction of global potential distribution and assessment of habitat suitability for *Xanthium spinosum* driven by climate change.

Front. Plant Sci. 16:1690546.
doi: 10.3389/fpls.2025.1690546

COPYRIGHT

© 2025 Fan, Zhang, Yang, Yang, Zhang, Yang and Li. This is an open-access article distributed under the terms of the Creative Commons Attribution License (CC BY). The use, distribution or reproduction in other forums is permitted, provided the original author(s) and the copyright owner(s) are credited and that the original publication in this journal is cited, in accordance with accepted academic practice. No use, distribution or reproduction is permitted which does not comply with these terms.

Prediction of global potential distribution and assessment of habitat suitability for *Xanthium spinosum* driven by climate change

Yuke Fan (b¹, Xiaowei Zhang (b², Junlong Yang (b¹, Jun Yang (b¹, Hongmei Zhang (b¹, Bo Yang (b¹) and Xiaowei Li (b^{1*})

¹College of Forestry and Prataculture, Ningxia University, Yinchuan, China, ²College of Forestry, Gansu Agricultural University, Lanzhou, China

Xanthium spinosum Linn (Asteraceae family), native to South America, is among the most invasive plant species globally, with major ecological, agricultural, and livestock-related impacts. However, little is known about how climate change may alter its future distribution and range shifts. This study assessed the potential global distribution and habitat suitability of X. spinosum by evaluating its dispersal risk under climate change. We compiled 13,378 global occurrence records and applied the MaxEnt model (optimized via the R package ENMeval) to simulate habitat suitability under current conditions and three future climate scenarios (SSP126, SSP370, and SSP585) for 2040-2060, 2060-2080, and 2080-2100. The model performed with high accuracy (area under the curve > 0.979). The most influential factor was the minimum temperature of the coldest month (Bio6; 67.1% contribution), with an optimal range of $-7.3\,^{\circ}\text{C}$ to $8.7\,^{\circ}\text{C}$. Other key drivers included Bio10, Bio19, and Bio7. Currently, core suitable areas include western North America to central/western Europe, southeastern South America to West Africa, and Southeastern Australia to East Asia, spanning $2,950.42 \times 10^4 \text{ km}^2$ (52.8% of potential distribution). Under SSP126, suitable habitats expand steadily ($+338.15 \times 10^4 \text{ km}^2$ by 2080–2100). SSP370 projects large fluctuations, peaking at $+ 448.26 \times 10^4$ km² in 2060–2080. SSP585 predicts rapid early expansion ($+392.54 \times 10^4$ km² by 2040–2060), with the rate of expansion decreasing in the mid and late stages. These findings support invasion risk assessment, early warning development, and targeted management strategies for X. spinosum in a changing climate.

KEYWORDS

alien invasive plants, *Xanthium spinosum*, climate change, potential distribution, species distribution models

1 Introduction

Invasive alien species are a critical component of global environmental change that pose substantial threats to national biosecurity, ecological security, and food security (Seebens et al., 2017; Van Kleunen et al., 2015; Guo et al., 2025). These invaders typically exhibit rapid growth, high resource use efficiency, strong dispersal capacity, and enhanced resistance to pathogens (Máximo et al., 2020). Through interference mechanisms, such as hybridization, alteration of natural habitats, and introduction of pathogenic organisms, they achieve a competitive advantage over native species, driving the latter toward decline or extinction, thereby occupying their ecological niches to facilitate selfexpansion (Baldi et al., 2022). Under intensifying global climate change, phenomena including warming climate, elevated atmospheric CO2 concentrations, increased nitrogen deposition, and frequent extreme climatic events have profoundly affected global ecosystem stability. Such changes drive species adaptation shifts, further exacerbating the dispersal risks of invasive alien species (Blackburn et al., 2011; Ren et al., 2022). Invasive plants are a primary cause of biodiversity loss. Compared with native flora, they exhibit significant competitive advantages in light acquisition, soil moisture utilization, and nutrient exploitation (Adkins and Shabbir, 2014; Karimmojeni et al., 2021). Once successfully established, highly adaptable and dispersive alien species trigger drastic declines in native biodiversity. Their effects extend beyond the direct displacement of indigenous species to fundamentally alter ecosystem structure and function, destroying habitats for multiple species and thereby posing severe threats to biodiversity (Zheng and Li, 2025).

Although native to subtropical South America, X. spinosum has become naturalized as a wild species across Central Europe, Southern Europe, the northwestern Pacific (Martin and Carnahan, 1983), Asia, and North America (Löve and Dansereau, 1959; Gligor et al., 2022). It is a toxic invasive annual weed (Wang et al., 2025) that is listed by the European Plant Protection Organization (EPPO) as a highly invasive plant species (EPPO Global Database, 2025). Its traits include extended flowering periods, high fecundity, prolific seed production, and strong cold tolerance (Yuan et al., 2018; Kelečević et al., 2024). Its seeds have hooked spines, which readily attach to livestock (e.g., cattle and sheep) and cargo, facilitating dispersal. This not only reduces the economic value of animal wool and hides but also drives large-scale spread of X. spinosum through adaptability to Mediterranean climates and affinity for nitrogen-rich soils (Andreani et al., 2017). X. spinosum has achieved global distribution (Weber, 2017), and the corresponding effects are particularly severe in ecologically fragile regions with simplified ecosystem structures (Wang et al., 2025). It suppresses native plants via allelopathy and, upon successful establishment, damages various crops (Liu et al., 2025). Consequently, it severely threatens biodiversity, agricultural production, and livestock farming in invaded areas while substantially increasing ecological restoration costs and economic management burden. Therefore, effective control of X. spinosum represents a major challenge.

The capacity of species to respond to climate change partly depends on their ability to disperse into suitable habitats, which are subject to climate change effects (Travis et al., 2013). Current research on invasive species indicate that climate change will considerably alter habitat suitability for invasive species, particularly considering the projected continuous increase in global mean temperatures through 2100 (Aidoo et al., 2025). The potential distribution of X. spinosum may shift, which is a critical question needing consideration. Consequently, predicting temporal changes in the potential distributions of invasive species is essential for effective management. Species distribution models (SDMs) can simulate future distribution scenarios, thereby support invasion risk reduction and optimizing conservation efforts (Guisan and Zimmermann, 2000); however, limited research on habitat suitability for X. spinosum hinders the formulation of early monitoring and prevention strategies. Previous studies have investigated X. spinosum primarily in terms of bio-ecological traits (Liu et al., 2025), invasion mechanisms and dispersal patterns (Xiao et al., 2023), isolation and identification of bioactive compounds, and allelopathic effects of secondary metabolites (Yuan et al., 2018). However, SDM-based predictions of suitable habitats for X. spinosum during climate change are scarce, with no existing global analysis. Therefore, projecting the climate-driven global geographic distribution patterns of *X. spinosum* is critically important.

SDMs serve as vital tools for studying how suitable habitats of species respond to climatic and environmental changes (Wiens et al., 2009; Hosseini et al., 2024). These models use geographic distribution data obtained from field surveys, herbarium records, and literature sources to infer the ecological niches of species. Based on the density patterns of occurrence points, they quantify the habitat preferences of species through probability estimates, thereby predicting the response of potentially suitable niches to climate change (Bellard et al., 2012). Commonly used SDM methods include bioclimatic envelope models (BIOCLIM) (Booth et al., 2014), maximum entropy (MaxEnt) models (Phillips et al., 2006), genetic algorithm for rule-set production models (Stockwell, 1999), generalized additive models (GAMs) (Hastie and Tibshirani, 1987), and generalized linear models (GLMs) (Nelder and Wedderburn, 1972; Beaumont et al., 2008). Among these models, the MaxEnt model demonstrates superior tolerance to sample bias and higher predictive accuracy compared with other models, yielding relatively optimal performance (Elith et al., 2006; Merow et al., 2014). Consequently, it has been widely used for predicting species distributions (Merow et al., 2013).

In this study, we elucidated the distribution patterns and dynamic changes of potentially suitable habitats for *X. spinosum*, providing scientific references for global invasion risk assessment, early warning systems, and management strategies. Under global climate change, we integrated global occurrence records of *X. spinosum* with multidimensional environmental factors. Using an optimized MaxEnt model (implemented via the R package ENMeval) combined with ArcGIS software, we simulated its potential suitable habitats under current conditions and three future periods (2040–2060, 2060–2080, and 2080–2100) across

three Shared Socioeconomic Pathways (SSP126, SSP370, and SSP585). Through regional-scale suitability classification and an analysis of key environmental drivers, the results identify current high-risk invasion hotspots, predict future habitat expansion trends, and inform targeted control measures, thereby offering critical scientific guidance for global management.

2 Materials and methods

2.1 Collection of species distribution data

Global distribution records of X. spinosum were compiled from multiple sources: the iNaturalist (iNat, https://www.inaturalist.org/), the Global Biodiversity Information Facility (GBIF, https:// www.gbif.org/), relevant literature. For specimen records lacking latitude and longitude coordinates, precise geographic coordinates were obtained using the Baidu Map Coordinate Picker System (http://api.map.baidu.com/lbsapi/getpoint/index.html). A preliminary total of 25,245 distribution records were collected (iNat: 4528; GBIF: 20,685; literature: 32). To ensure high-quality data, a rigorous screening of the raw records was performed. Records with errors, those falling outside of the species' actual distribution range, or those lacking specific geographic information were excluded. Because data from different sources (databases, literature) may exhibit spatial clustering (i.e., multiple records at adjacent locations), which can easily cause spatial autocorrelation in SDMs, leading to model overfitting and reduced predictive accuracy (Teng et al., 2018), we applied spatial thinning to the data using the ENMTools package in R (Warren et al., 2021). In particular, only one unique distribution point was retained within a 20-km radius. This mitigated spatial autocorrelation and considerably improved the accuracy of the model predictions for the potential suitable geographic distribution of X. spinosum. Ultimately, 9,134 valid distribution points with latitude and longitude data were obtained. These data were organized, imported into Excel, and saved in CSV format for subsequent model construction.

2.2 Collection of environmental variables and setting of future climate scenarios

This study incorporated two categories of environmental variables: climate and soil are shown in Table 1. Nineteen bioclimatic variables (Bio1-Bio19) were sourced from the WorldClim 2.1 database (https://worldclim.org/) at a spatial resolution of 2.5 arc-minutes. Ten soil factors were obtained from the Harmonized World Soil Database (HWSD) v2.0 (https://www.fao.org/). After model construction, the projections of the potential suitable habitats of *X. spinosum* under future climate scenarios (2040–2060, 2060–2080, and 2080–2100) used future-period climate data while maintaining current soil conditions. All environmental layers were standardized to 2.5 arc-minute resolution. Because CMIP6 (Coupled Model Intercomparison

Project Phase 6) integrates Shared Socioeconomic Pathways (SSPs) with socioeconomic factors, considerably enhancing the scientific robustness of future simulations (Popp et al., 2017; Khadka et al., 2022), we adopted future bioclimatic data from the EC-Earth3 climate model under CMIP6, which is well-regarded for simulations over European regions. Three representative SSP scenarios were selected to reflect progressively elevated carbon emissions: SSP126 (Sustainable Development Pathway), SSP370 (Intermediate Development Pathway), and SSP585 (Rapid Development Pathway).

2.3 Environmental variable screening

High correlations among environmental variables can result in overfitting in MaxEnt model results, which compromises the accuracy of variable contribution rates and predicted species distribution ranges (Evans et al., 2010). We implemented the following screening protocol: Preliminary Contribution Screening: All environmental variables were imported into MaxEnt 3.4.4. After 10 replicated runs (cross-validation), the variables were ranked based on their average contribution rates. Variables with a zerocontribution rate were excluded. Multicollinearity Check: Pearson correlation coefficients among retained variables were calculated using the raster package in R, as shown in Figure 1. Variables were retained only if absolute correlation coefficients were below 0.8 (|r| < 0.8). For variable pairs with $|r| \ge 0.8$, only the variable exhibiting a higher contribution rate was retained (Sharma et al., 2018). Through this process, 14 environmental variables were ultimately selected for modeling.

2.4 MaxEnt model parameter optimization

Using default parameters for habitat prediction across species increases model sensitivity to sampling bias and risks overfitting, thus compromising prediction reliability. Regularization Multiplier (RM) and Feature Class (FC) influence model complexity and predictive accuracy. RM determines model complexity, while FC governs potential shapes of marginal response curves (Phillips et al., 2017). To enhance prediction precision, we used the ENMeval package in R to optimize RM and FC parameters. Model complexity was evaluated using corrected Akaike Information Criterion (AICc) values under different parameter combinations, with those yielding the lowest complexity selected for modeling (Muscarella et al., 2014). Default settings included RM = 1. Standard FC selection proceeded as follows: Linear (L) features always included, Quadratic (Q) features enabled at ≥ 10 occurrence points, Hinge (H) features enabled at ≥ 15 points, Threshold (T) and Product (P) features enabled at \geq 80 points (West et al., 2016). We tested RM values from 0.5 to 4 (increments of 0.5) and six FC combinations: H, L, LQ, LQH, LQHP, and LQHPT. Based on R analysis, optimized parameters were set to RM = 0.5 and FC=LQ for final model execution as shown in Figure 2.

TABLE 1 Description of environmental variables.

Туре	Field	Description and unit	Туре	Field	Description and unit		
Climatic	Bio1	Annual mean temperature °C		Bio16	Precipitation of the wettest quarter (mm)		
factors	Bio2*	Mean diurnal range °C		Bio17*	Precipitation of the driest quarter (mm)		
	Bio3*	Isothermality		Bio18*	Precipitation of the warmest quarter (mm)		
	Bio4	Temperature seasonality		Bio19*	Precipitation of the coldest quarter (mm)		
	Bio5	Max temperature of the warmest month °C	Soil factors	t-Ece	Soil conductivity dS/m		
	Bio6*	Min temperature of the coldest month °C		t-Clay	Clay content %wt		
	Bio7*	Temperature annual range °C		t-Cec-Clay	Soil cation exchange content cmol/		
	Bio8*	Mean temperature of the wettest quarter °C		t-CaSO ₄ *	Soil sulfate content %weight		
	Bio9*	Mean temperature of the driest quarter °C		t-CaCO ₃ *	Soil carbonate content %weight		
	Bio10*	Mean temperature of the warmest quarter °C		t-Gravel	Soil gravel content %vol.		
	Bio11	Mean temperature of the coldest quarter °C		t-Sand	Sand content %wt.		
	Bio12*	Annual precipitation (mm)		t-Silt	Silt content %wt.		
	Bio13	Precipitation of the wettest month (mm)		t-Teb	Soil exchangeable salts cmol/kg		
	Bio14	Precipitation of the driest month (mm)		t-Esp	Exchangeable sodium salt %		
	Bio15*	Precipitation seasonality		t-Texture	Topsoil texture		

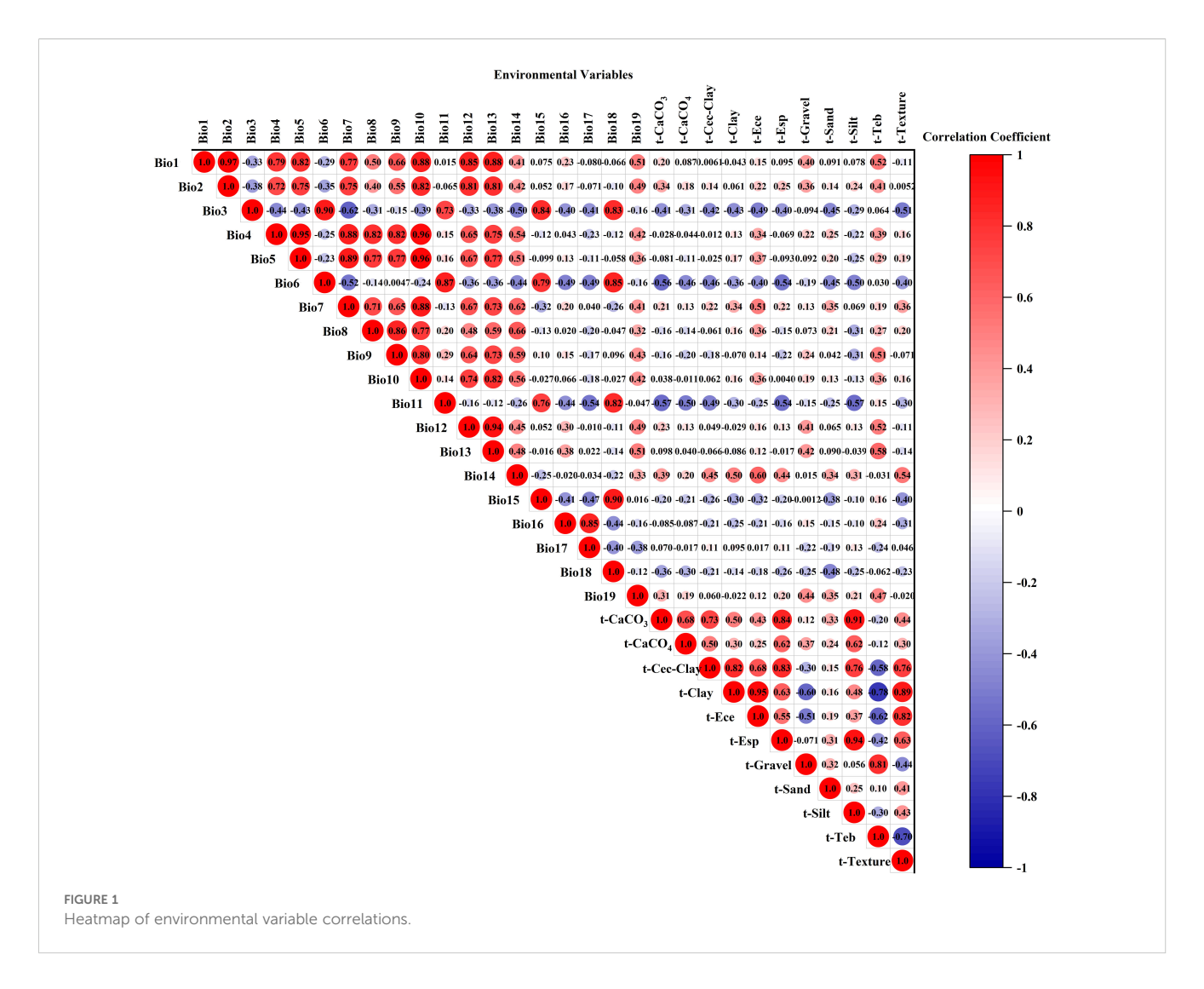
 $Environmental\ factors\ marked\ with\ *\ are\ variables\ used\ in\ MaxEnt\ model\ predictions.\ Attributes\ prefixed\ with\ "t-"\ represent\ upper\ soil\ attributes\ (0-30\ cm).$

2.5 Model training and accuracy evaluation

Following data preparation and model optimization, 13,378 screened distribution points and 14 environmental variables were entered into the optimized MaxEnt model (Version 3.4.4). The dataset was partitioned with 75% of samples for training and 25% for testing (Zhang et al., 2018). Climate variable importance was quantified via jackknife tests and contribution rates (Wan et al., 2019). Model Parameters: maximum background points: 10,000 maximum iterations: 5,000 10-replicate runs to reduce stochastic error (Santana et al., 2019), model performance was evaluated using the AUC of the receiver operating characteristic (ROC) (Liu et al., 2021). AUC values range from 0 to 1, with predictive accuracy classified as Unacceptable (0.50—0.70), Moderate (0.70—0.80), Good (0.80—0.90), Excellent (0.90—1.00) (Araújo et al., 2005), identical parameter configurations were applied for future scenario projections.

2.6 Delineation of potential suitable habitats and distribution dynamics

Habitat suitability probabilities derived from the optimized MaxEnt model were classified into suitability levels using the Natural Breaks method (minimizing within-group variance, while maximizing between-group variance) (Ke et al., 2023) in ArcGIS 10.8. Based on the observed distribution of X. spinosum, four suitability classes were defined: Unsuitable (0.00–0.10), Low suitability (0.10–0.33), Moderate suitability (0.33–0.64), and High suitability (0.64–1.00). Identical thresholds were applied to future scenarios. Areas with an occurrence probability \geq 0.33 demonstrated a higher likelihood of species survival (Zhang et al., 2025). Consequently, moderate and high suitability zones were combined as core suitable habitats. The Reclassify tool in ArcGIS quantified areal extents of each suitability class per scenario. Regions with an occurrence probability >0.10 were mapped as potential distribution areas.



Species probability maps (0–1 scale) were converted to binary presence/absence maps (0/1) using the ArcGIS con function, with thresholds determined by sensitivity–specificity optimization (Li et al., 2020). Within ArcGIS, the SDMtoolbox 2.5 extension was used to classify habitat dynamics into expansion, stability, and contraction, calculate centroid coordinates for future periods, and trace centroid migration trajectories relative to current conditions.

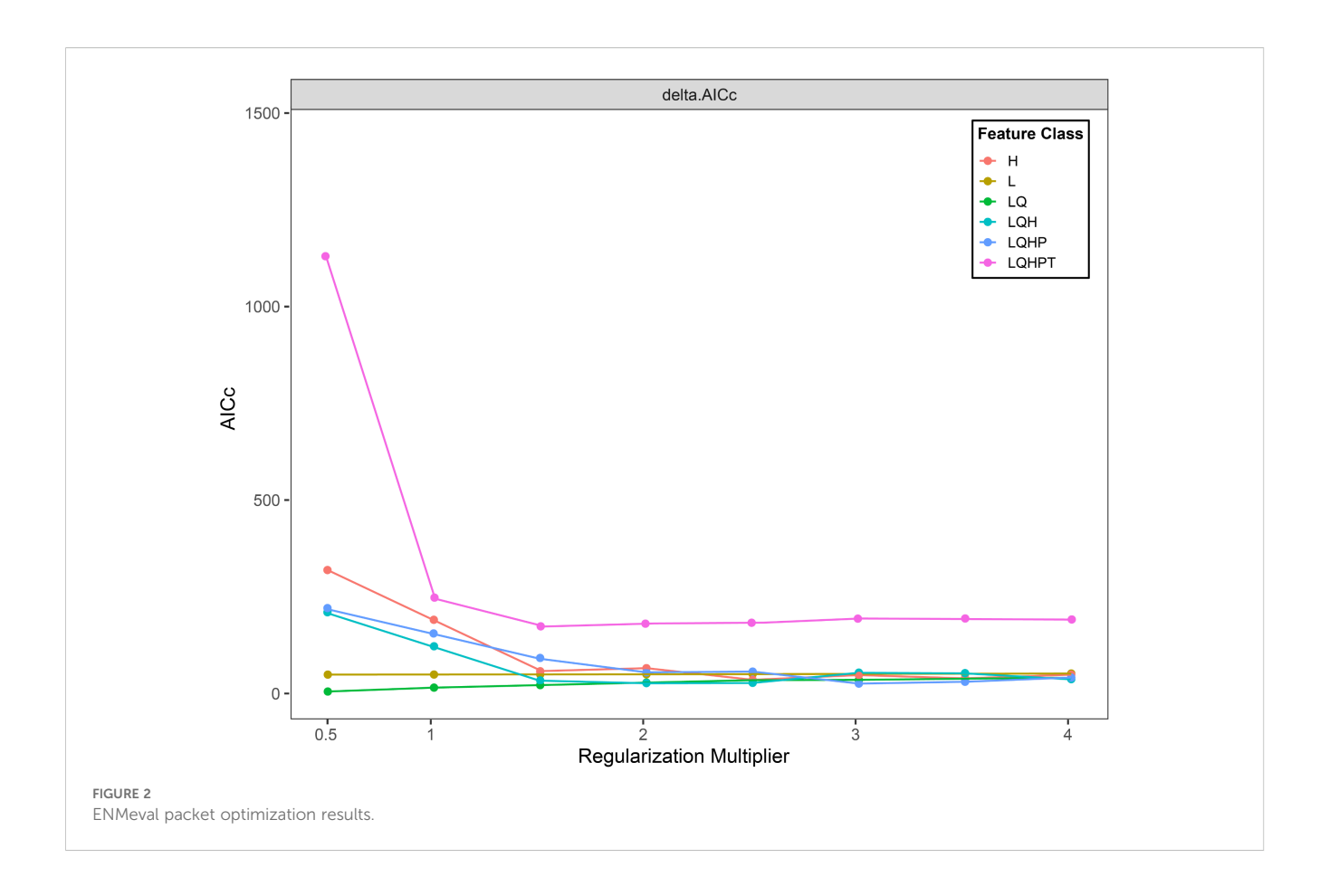
3 Results and analysis

3.1 Model predictions and performance evaluation

Model accuracy depends on sample coverage, with AUC representing the optimal evaluation metric (Hosseini et al., 2024). The optimized MaxEnt model simulated the distribution of *X. spinosum* showed that the AUC value of the model training set reached 0.979, as shown in Figure 3. These results indicate excellent model fit and a robust predictive capacity for the potential habitats of *X. spinosum*, which confirms the model's reliability for projecting future distributions.

3.2 Dominant factors in habitat suitability

This study analyzed the contributions of environmental variables to model construction are shown in Table 2. Based on the percent contribution, the top three key variables influencing X. spinosum distribution were Minimum Temperature of Coldest Month (Bio6, 67.1%), Precipitation of Coldest Quarter (Bio19, 21.8%), and Mean Temperature of Warmest Quarter (Bio10, 4.1%). These three variables collectively accounted for 93.0% of the total contribution, with Bio6 alone contributing 67.1%, highlighting the dominant role of bioclimatic variables. Jackknife tests further validated variable importance, as shown in Figure 4. The results indicated that for light green bars (single variable), higher training gain indicates greater information content and stronger influence on species distribution. For dark green bars (excluding single variables), lower training gain signifies greater uniqueness and importance of the removed variable. Based on the jackknife evaluation of regularized training gain and test gain, the three most critical variables affecting X. spinosum distribution were Minimum Temperature of Coldest Month (Bio6), Mean Temperature of Warmest Quarter (Bio10), and Temperature



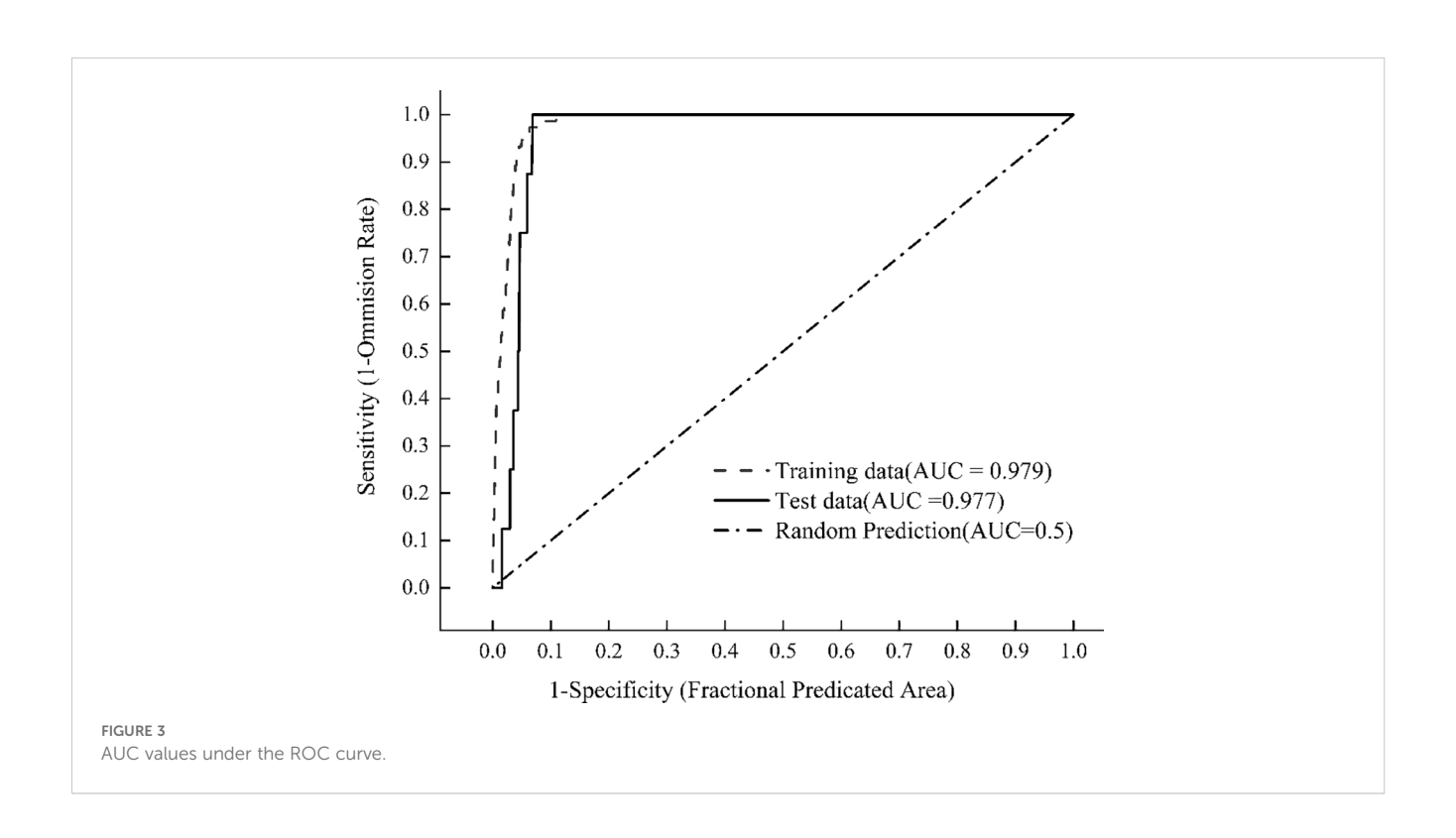


TABLE 2 Percent contribution of key environmental variables.

Code	Current/ %	2040—2060/%			2060—2080/%			2080—2100/%		
Code		SSP126	SSP370	SSP585	SSP126	SSP370	SSP585	SSP126	SSP370	SSP585
Bio6	67.1	68.9	61.2	65.1	69.8	57.4	58.9	66.2	61.2	65.8
Bio19	21.8	20.1	20.9	19.5	17.0	20.9	23.7	17.3	22.9	16.5
Bio10	4.1	4.2	5.1	4.8	5.3	3.3	5.3	4.2	6.1	4.2
Bio7	1.3	0.9	1.2	1.0	2.2	1.2	2.3	2.5	2.2	1.7

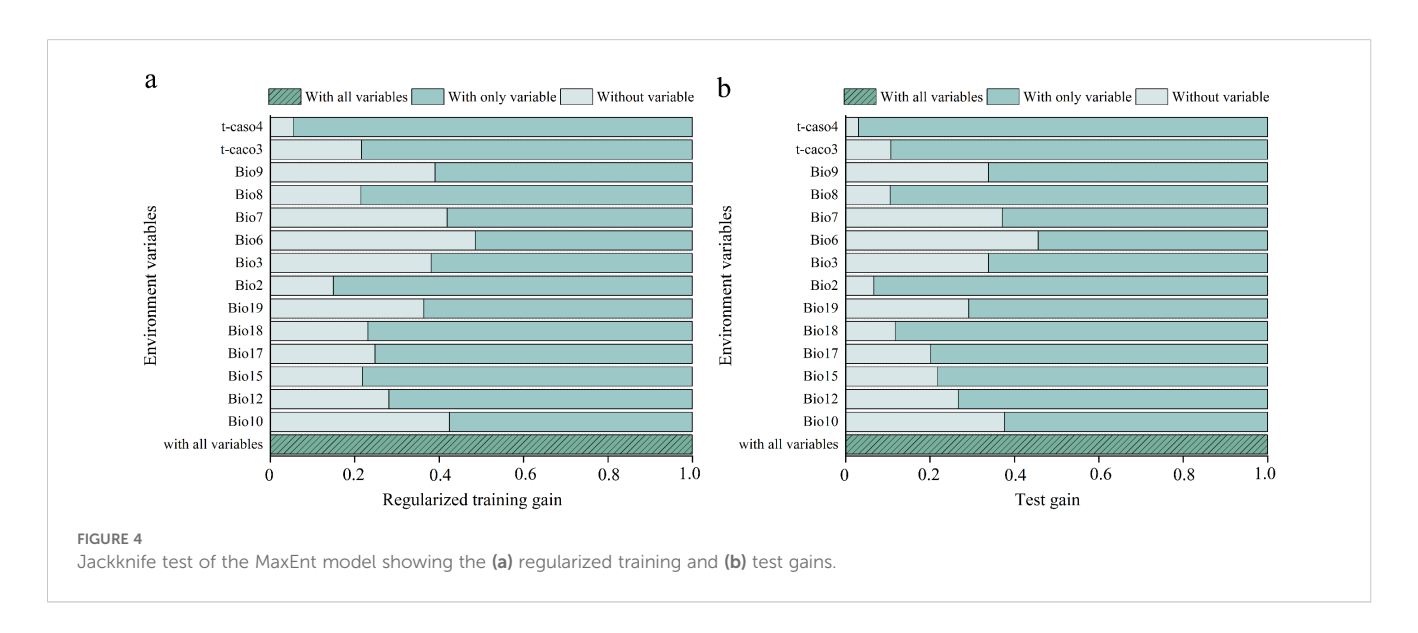
Annual Range (Bio7). Synthesis of percent contribution and jackknife results demonstrated that bioclimatic variables (Bio6, Bio10, Bio19, Bio7) overwhelmingly dominated soil factors in MaxEnt predictions of *X. spinosum* distribution. Bio6 (Minimum Temperature of Coldest Month), Bio10 (Mean Temperature of Warmest Quarter), Bio19 (Precipitation of Coldest Quarter), and Bio7 (Temperature Annual Range) were identified as the key environmental variables for predictive modeling, with Bio6 being the dominant factor because of its significantly higher contribution rate.

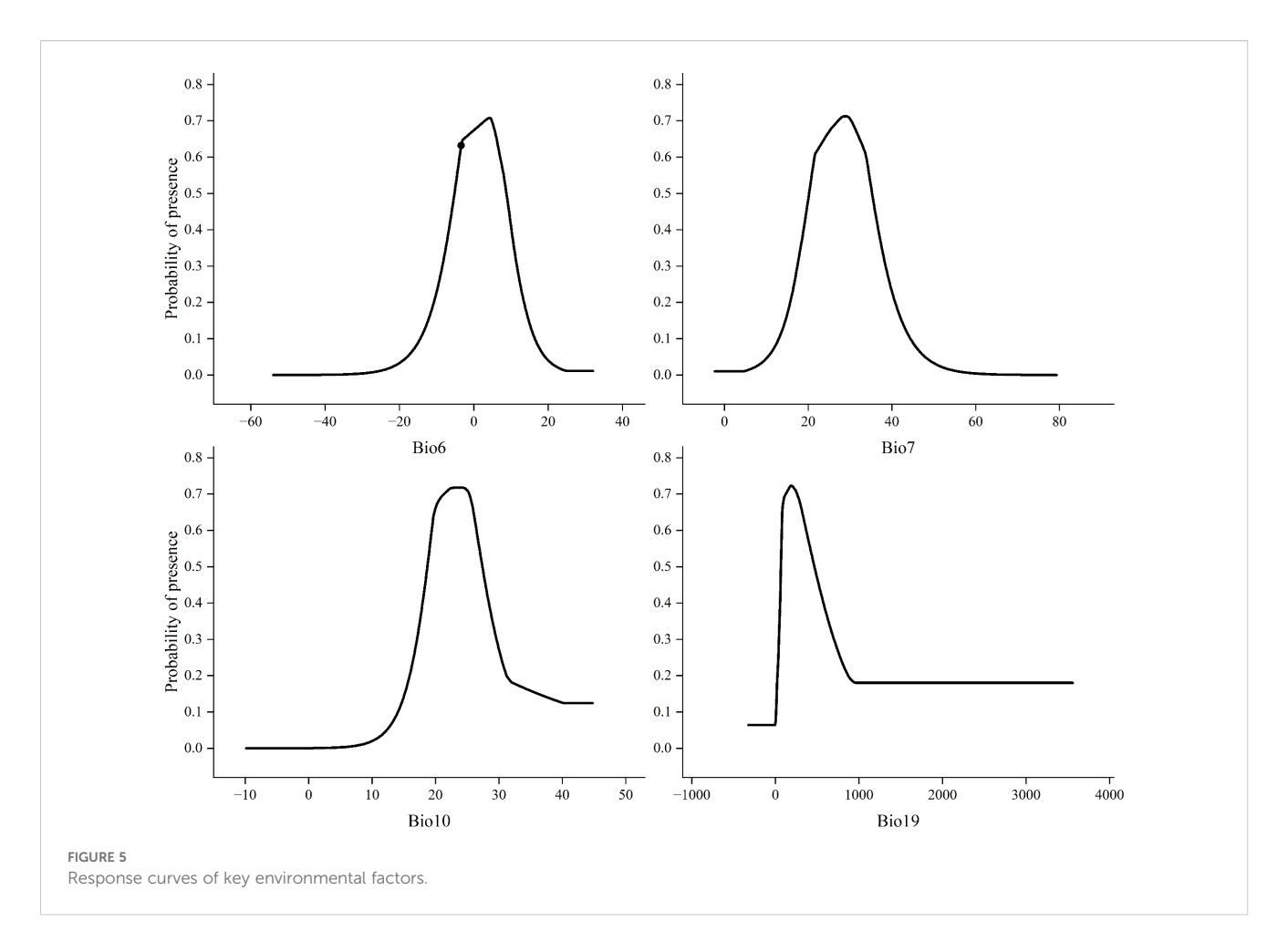
By analyzing the response curves of environmental factors, the relationship between the survival probability of the target species and specific environmental factors can be determined. A higher survival probability (P) is more conducive to the survival of the species (Zhang et al., 2025). This study defines areas with a survival probability of >0.64 as highly suitable habitats. Therefore, this threshold indicates that the corresponding combination of environmental factors is more favorable for the growth of the species. Analysis of the response curves for the four key environmental factors (Bio6, Bio7, Bio10, Bio19), as shown in Figure 5 showed the Minimum Temperature of the Coldest Month (Bio6): The suitable range for X. spinosum survival (P > 0.64) was -7.3°C to 8.7°C. Survival probability drops below 0.64 when temperatures fall below -7.3°C or rise above 8.7°C. Its optimal growth temperature is approximately 4.2°C (where P peaks). Temperature Annual Range (Bio7): The suitable survival

threshold was -22.4°C to 33.2°C. The optimal value was approximately 27.5°C (where P peaks). Mean Temperature of Warmest Quarter (Bio10): The suitable range was narrower (18.3°C to 24.6°C). The optimal temperature was approximately 24.8°C (where P peaks). Precipitation of the Coldest Quarter (Bio19): The suitable range was wider (83.45 mm to 421.83 mm). The optimal precipitation was approximately 207.8 mm (where P peaks).

3.3 Suitable habitat distribution of *Xanthium spinosum* under the current climatic scenario

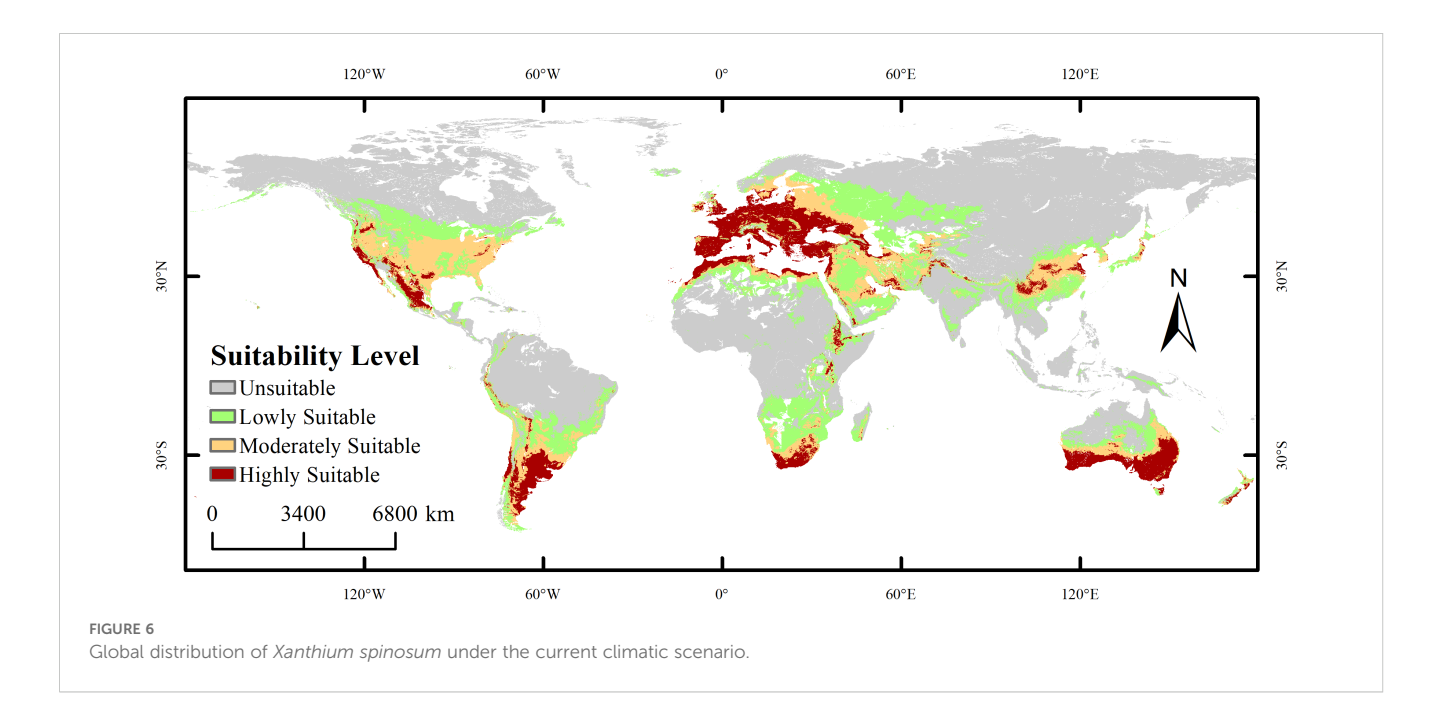
Under current climatic conditions, the suitable habitat of the species exhibits a significant spatial differentiation pattern, as shown in Figure 6. The potential distribution area of *X. spinosum* (occurrence probability >0.1) is widely distributed across central to western North America (120°W–60°W), northern to southeastern South America (60° W–0°), central–western Europe (0°–60°E), central to West Africa (0°–40°E), inland to coastal Asia (60°E–120°E), and southeastern Australia (120°E–180°E), to form a continuous distribution belt spanning five continents, with a total area of $5,620.18 \times 10^4$ km². The highly suitable habitat (area $1,380.65 \times 10^4$ km²) exhibits a fragmented, patchy, and banded distribution pattern, with core concentrations near 30°N in $120^\circ\text{W}-60^\circ\text{W}$ (western North America) and $0^\circ-60^\circ\text{E}$ (central–western





Europe), and near 40°S in 120°E–180°E (southeastern coastal Australia). The moderately suitable habitat (1,569.77× 10^4 km²), serving as a transition zone surrounding the highly suitable areas, is mainly distributed in $60^\circ\text{W}-0^\circ$ (southeastern South America, West

Africa) and 60°E–120°E (coastal East Asia and eastern India), showing locally contiguous features. The lowly suitable habitat $(2,669.76\times10^4 \text{ km}^2)$ extensively and continuously covers central North America (60° W–120°W), northern South America (60°W–0°), central Africa (0°–



 40°E), and inland Asia ($60^{\circ}\text{E}-120^{\circ}\text{E}$). The unsuitable habitat ($8,473.62\times10^4~\text{km}^2$) is widely distributed in high-latitude polar regions (> 40°N/S), arid inland areas (e.g., western North America, Central Asia), and core tropical rainforest zones ($0^{\circ}-10^{\circ}$ latitude).

3.4 Changes in global distribution under three future climate scenarios

Under the three future climate scenarios (SSP126, SSP370, SSP585), the spatial pattern of suitable habitats for *X. spinosum* undergoes significant changes, with a pronounced displacement of the distribution centroid, as shown in Figure 7. Overall, the total suitable habitat area expands compared with the current climate scenario, whereas the core suitable habitat (highly suitable area) generally contracts.

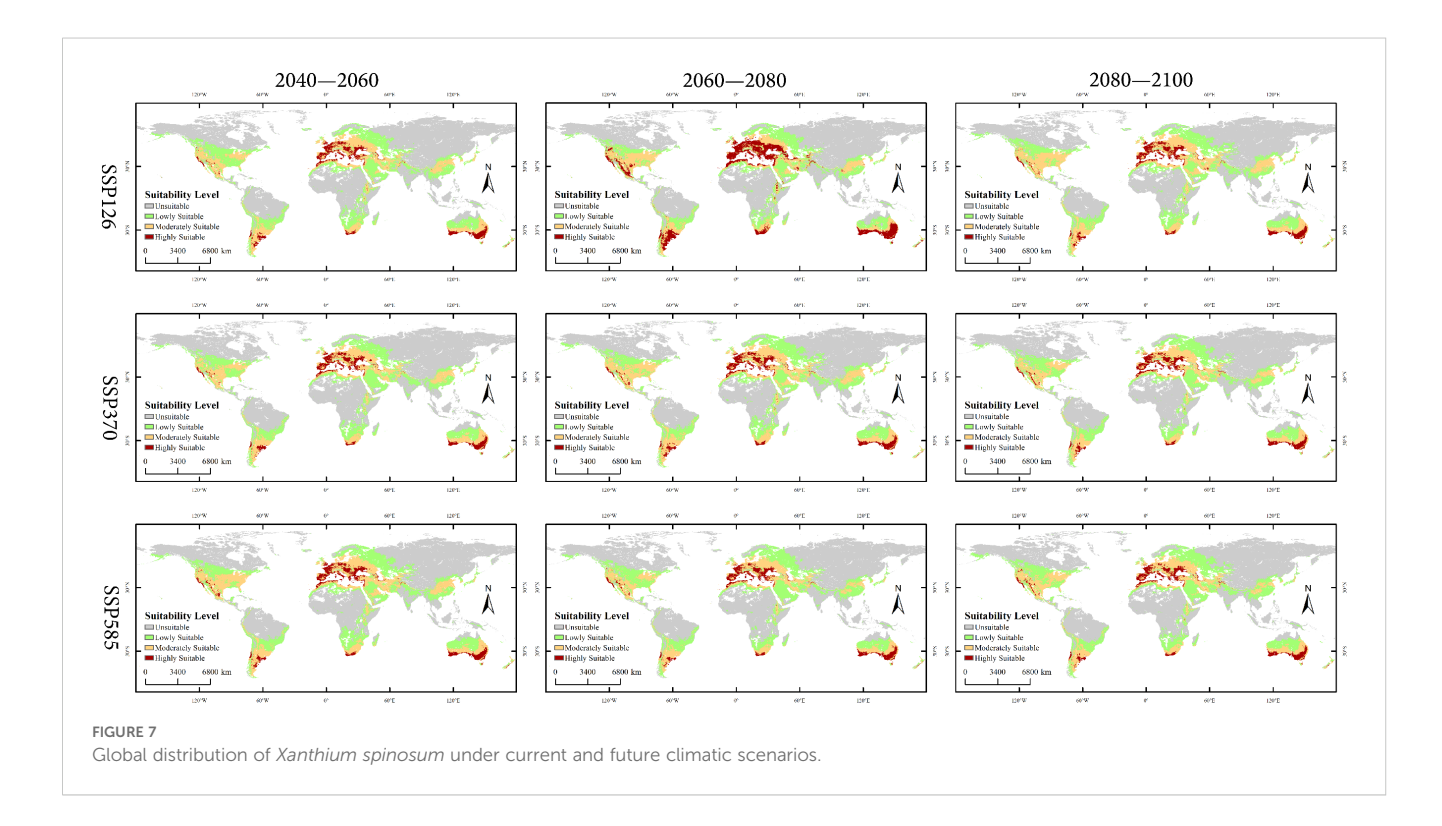
Low-emission pathway (SSP126): The suitable habitat area continuously expands over time, with the net increase rising from 170.18×10^4 km² in 2040–2060 to 338.15×10^4 km² in 2080–2100, as shown in Figure 8. The core suitable habitat area exhibits the most significant reduction initially (-495.32×10^4 km²). The stable area decreases slightly in the mid-term (-4.77%), recovering to 5105.61×10^4 km² by the end-term, as shown in Figure 9, Table 3. Medium-emission pathway (SSP370): The suitable habitat area change shows strong fluctuations. The net change shifts from an early increase ($+89.74 \times 10^4$ km²) to a peak expansion during the mid-term ($+448.26 \times 10^4$ km²), then returns to an increase by the end-term ($+82.56 \times 10^4$ km²). The core suitable habitat area exhibits the most pronounced reduction initially (-535.21×10^4 km²). The stable area begins to expand from the mid-term ($+151.17 \times 10^4$ km²), but decreases slightly by the end-term (-0.70%), with the

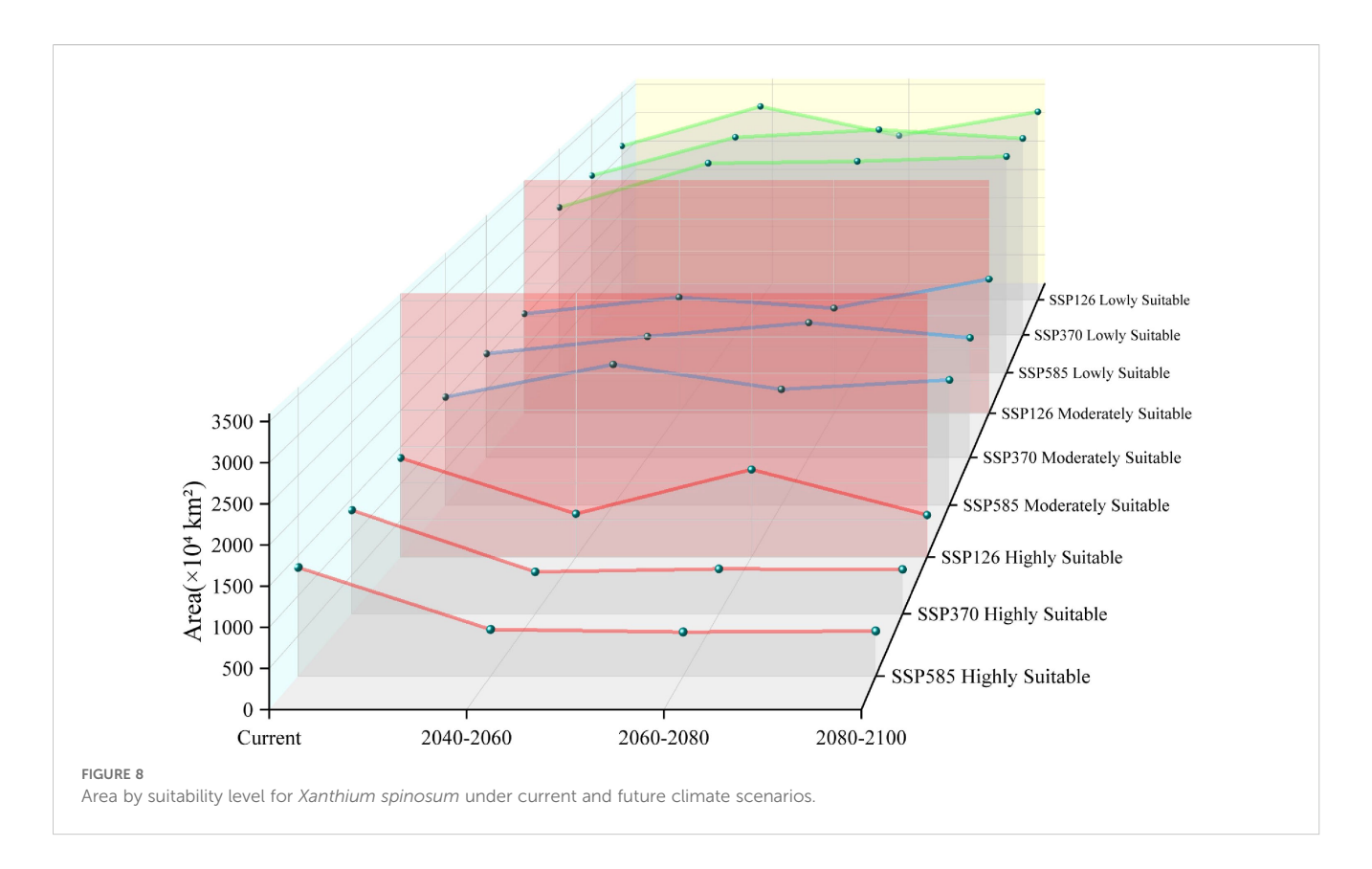
2080–2100 stable area being 4905.94 × 10^4 km². Under the highemission pathway (SSP585), suitable habitat area has an early peak in net increase (+392.54 × 10^4 km²), exhibits a sharp slowdown in expansion mid-term (+46.85 × 10^4 km²), and returns to an increase by the end-term (+265.38 × 10^4 km²). The stable area continuously decreases; the largest reduction occurs mid-term (-4.00%) and the area shrinks to 4995.85 × 10^4 km² by the end-term.

4 Discussion

4.1 Dominant factors influencing the distribution of *Xanthium spinosum*

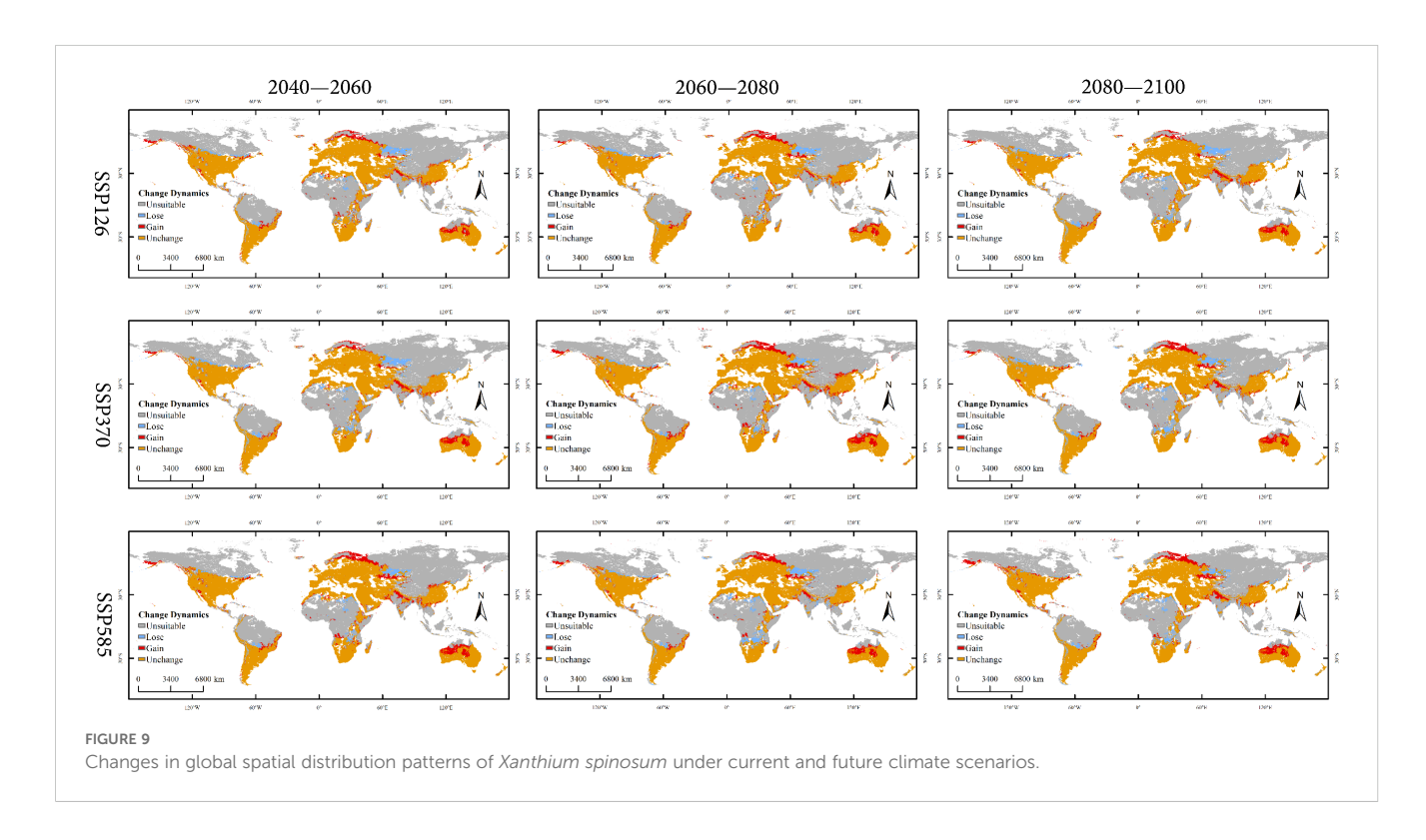
In this study, we used the MaxEnt model optimized through the R package ENMeval to simulate the potential distribution of X. spinosum under current and future periods (2040–2060, 2060–2080, and 2080-2100) across three climate scenarios (SSP126, SSP370, and SSP585). By comprehensively analyzing the contribution rates and training gain values of dominant climatic factors and plotting their response curves, we quantified the environmental characteristics of the natural distribution of X. spinosum and analyzed its suitable growth conditions. Results indicated that under current climatic conditions, temperature and precipitation are the predominant environmental variables that determine the distribution of X. spinosum, with temperature being particularly important as the dominant factor controlling its invasive spread (Gallardo et al., 2015). Among the environmental factors included in the model, Bio6 (Min Temperature of Coldest Month), Bio7 (Temperature Annual Range), Bio10 (Mean Temperature of Warmest Quarter), and Bio19 (Precipitation of Coldest Quarter)





considerably influenced species distribution. Three of these four factors are temperature-related (Bio6, Bio7, Bio10), and Bio6 exhibited the highest contribution rate, indicating that temperature factors contribute more substantially to the geographical distribution of X. spinosum than precipitation. This

is consistent with the ecological traits of the species including strong adaptability to desert environments and low water requirements (Andreani et al., 2017). Simulation predictions reveal that under future climate scenarios, Bio6 remains the dominant climatic factor that limits the potential suitable habitat for *X. spinosum*. Optimal



Change	2040—2060 × 10 ⁴ km ²			2060-	–2080 × 10 ²	2080—2100 × 10 ⁴ km ²			
Dynamics	SSP126	SSP370	SSP585	SSP126	SSP370	SSP585	SSP126	SSP370	SSP585
Lose	402.15	445.28	310.65	480.14	325.42	505.73	327.59	523.18	419.37
Gain	572.33	558.46	655.39	485.68	776.12	591.46	722.44	571.82	687.93
Unchanged	5217.85	4968.57	5105.61	4940.67	5091.84	4905.94	5093.76	4889.66	4995.85

TABLE 3 Changes in global suitable habitat area of Xanthium spinosum under current and future climate scenarios.

seed germination for X. spinosum occurs near 25 °C (Auld, 1993), whereas germination of the congeneric Xanthium strumarium is inhibited above 35 °C and shows a sharp decline in germination rate (Saeed et al., 2020). Our response curve analysis is consistent with these findings: The optimal Mean Temperature of Warmest Quarter (Bio10) for X. spinosum growth is approximately 24.8 °C, and its survival threshold for Temperature Annual Range (Bio7) spans -22.4 °C to 33.2 °C, beyond which survival probability decreases. X. spinosum exhibits strong adaptability to Mediterranean climates (Andreani et al., 2017). Our results indicate that, under climate change, this species is likely to further expand into Mediterranean regions. As precipitation is concentrated during the cold season in most Mediterranean climates (Moore et al., 2020), and precipitation significantly influences seedling emergence, survival, and establishment of annual herbs (Wang and Gou, 2019), this study confirms that precipitation in the coldest quarter (Bio19) is a key environmental factor determining its distribution. In addition, X. spinosum exhibits broad tolerance for Precipitation of Coldest Quarter (Bio19) (69-458 mm), reflecting its strong adaptability to arid and humid environments, which is consistent with its inherent stress-tolerant traits (Tao et al., 2022).

4.2 Distribution pattern under current climatic conditions

This study reveals the dynamic response of suitable habitats for X. spinosum to climate change on a global scale. Currently, the core suitable habitat is concentrated in three regions: the western North America-central-western Europe corridor (120°W-60°W and 0°-60°E), the southeastern South America-West Africa transition zone (60°W-0° and 0°-20°E), and the southeastern Australia-East Asia coastal chain (120°E-180°E extending to 60°E-120°E), totaling 2,950.42×10⁴ km² (52.8% of the potential distribution area). This finding aligns closely with documented occurrence records (Güez et al., 2012; Lin et al., 2014), while simultaneously validating the reliability of MaxEnt for modeling the habitat suitability of X. spinosum. This broad adaptability enables establishment of the population in barren soils (e.g., moderately suitable areas in southeastern South America); however, the complete absence in core tropical rainforest zones (0°-10° latitude; unsuitable habitat covers 58.0% of these areas) indicates that high humidity and shaded environments constitute dispersal barriers. Furthermore, plant invasions are often closely associated with human activities. The seeds of X. spinosum possess a barbed structure on their surface; this facilitates unintentional dispersal through human activities and adheres to animal fur, enabling rapid expansion and colonization across extensive areas (Auld et al., 1988; Hocking and Liddle, 1986). In contrast, regions such as arid deserts, cold polar zones, and pristine tropical rainforests exhibit limited human activities owing to their extreme climates, complex topography, and remote location (Goosse et al., 2018; Zhang et al., 2018; Batterbury and Forsyth, 1999). Our findings also indicate that these regions for example the Sahara Desert and large parts of South American tropical rainforests, are classified as unsuitable distribution areas; this may also be related to the relatively low intensity of human activities in these regions.

4.3 Distribution patterns under future climate scenarios

Climate change impacts ecosystem stability by altering temperature and precipitation patterns, which potentially create new invasion opportunities for alien species, such as X. spinosum. Simulations using the optimized MaxEnt model indicate an expansion in the total suitable habitat area of X. spinosum across all future climate scenarios, which are consistent with predictions by Liu et al (Liu et al., 2025). for its distribution in China. Although total suitable area expands un0der all three scenarios, the core suitable habitat area decreases across all scenarios, particularly during early stages (e.g., reductions of 508.75×10⁴ km² under SSP126 and 548.76×10⁴ km² under SSP370). This phenomenon may relate to intensified climate change under global warming, including increased extreme heat events (Tang et al., 2025) and altered precipitation patterns (Rupp et al., 2022), which shifts environmental conditions away from the optimal growth requirements of X. spinosum, thereby contracting core habitats. These results are consistent with concerns that climate change exacerbates biodiversity loss and ecosystem vulnerability (Anderson, 2013; Marzloff et al., 2018).

X. spinosum is known for its high adaptability and reproductive capacity (Li and Ma, 2019). Its invasion into new regions poses severe management challenges (Gligor et al., 2022). The results of this study indicate that future contraction of suitable areas will be primarily concentrated in regions with high aridity and projected decreases in precipitation; for example, northern Kazakhstan and large parts of Africa (Teleubay et al., 2023; Nooni et al., 2022). As global warming exacerbates drought conditions, these areas may exceed the physiological tolerance range of *X. spinosum*, leading to a significant reduction in suitable habitats. In contrast, the expansion

of suitable areas will occur mainly in high-latitude northern regions, such as western Russia, and areas where future precipitation is expected to increase, such as northwestern Australia (Watterson et al., 2016; Cullen and Grierson, 2007). Global climate warming, particularly the rise in the minimum temperature of the coldest month (bio6), is projected to facilitate the spread of *X. spinosum* into higher latitude regions. Consequently, particular attention should be given to the invasion risk of *X. spinosum* in northern high-latitude zones and other areas where future climate projections indicate that there will be both suitable temperatures and increased precipitation.

4.4 Limitations and future prospects

This study examines the suitable habitat patterns of *X. spinosum* by analyzing environmental factors and geographic distribution. Our model mainly incorporates climatic and soil variables, as climate is widely recognized as a key driver of species distribution (Pacifici et al., 2017), and soils in high-latitude regions may further constrain plant migration (Ni and Vellend, 2024). These variables are generally considered fundamental in shaping species distributions (Ulrich et al., 2014). However, there remains limited research on the biological interactions of *X. spinosum* and the effects of human activities under future climate scenarios. Despite this gap, the model developed in this study, based on environmental similarity principles (Elith et al., 2011), offers meaningful projections. Future studies should integrate biotic interactions and anthropogenic factors as predictors to better simulate potential invasion areas and provide more precise support for global biosecurity governance.

5 Conclusion

In this study, we used an optimized MaxEnt model to predict the global potential distribution pattern of X. spinosum under climate change. The main conclusions are as follows: The Min Temperature of Coldest Month (Bio6) is the core climatic factor determining the current global distribution of X. spinosum (contribution rate of 67.1%), with a suitable range of -7.3°C to 8.7°C. Under three future emission scenarios (SSP126, SSP370, and SSP585), Bio6 remains the most critical limiting factor. Under current climate conditions, the potential suitable habitat of X. spinosum is primarily distributed in the central to western regions of North America (120°W-60°W), the northern to southeastern regions of South America (60°W-0°), the central to western regions of Europe (0°-60°E), the central to western regions of Africa (0°-40°E), inland to coastal Asia (60°E-120°E), and southeastern Australia (120°E-180°E). The total area of the potential suitable habitat is approximately $5,620.18 \times 10^4 \text{ km}^2$, with the core suitable habitat covering 2,950.42 × 10⁴ km². Under three future climate scenarios, the potential suitable habitat area of X. spinosum shows an expanding trend, whereas the core suitable habitat area shows a shrinking trend. The significant reduction in future suitable areas may be related to the decreased precipitation in these regions.

Data availability statement

The original contributions presented in the study are included in the article/supplementary material. Further inquiries can be directed to the corresponding author.

Author contributions

YF: Writing – original draft, Writing – review & editing. XZ: Supervision, Writing – review & editing. JLY: Supervision, Writing – review & editing. JY: Formal analysis, Writing – review & editing. HZ: Conceptualization, Investigation, Writing – review & editing. BY: Investigation, Writing – review & editing. XL: Investigation, Methodology, Supervision, Writing – review & editing.

Funding

The author(s) declare financial support was received for the research and/or publication of this article. This research work was supported by grants from the Ningxia Helan Mountains Vegetation Survey Project (2025), the Inner Mongolia Helan Mountains National Nature Reserve Scientific Expedition Project (2023), and the Ningxia Higher Education First-Class Discipline Construction (Grass Science) Project (NXLXK2017A01).

Conflict of interest

The authors declare that the research was conducted in the absence of any commercial or financial relationships that could be construed as a potential conflict of interest.

Generative AI statement

The author(s) declare that no Generative AI was used in the creation of this manuscript.

Any alternative text (alt text) provided alongside figures in this article has been generated by Frontiers with the support of artificial intelligence and reasonable efforts have been made to ensure accuracy, including review by the authors wherever possible. If you identify any issues, please contact us.

Publisher's note

All claims expressed in this article are solely those of the authors and do not necessarily represent those of their affiliated organizations, or those of the publisher, the editors and the reviewers. Any product that may be evaluated in this article, or claim that may be made by its manufacturer, is not guaranteed or endorsed by the publisher.

References

Adkins, S., and Shabbir, A. (2014). Biology, ecology and management of the invasive parthenium weed (*Parthenium hysterophorus L.*). *Pest Manag Sci.* 70, 1023–1029. doi: 10.1002/ps.3708

Aidoo, O. F., Amaro, G. C., Souza, P. G. C., Picanço, M. C., Awuah-Mensah, K. A., and Silva, R. S. (2025). Climate change impacts on worldwide ecological niche and invasive potential of *Sternochetus mangiferae*. *Pest Manag Sci.* 81, 667–677. doi: 10.1002/ps.8465

Anderson, R. P. (2013). A framework for using niche models to estimate impacts of climate change on species distributions. *Ann. N Y Acad. Sci.* 1297, 8–28. doi: 10.1111/nvas.12264

Andreani, S., Paolini, J., Costa, J., and Muselli, A. (2017). Chemical composition of essential oils of *Xanthium spinosum* L., an invasive species of Corsica. *Chem. Biodivers* 14, 1600148. doi: 10.1002/cbdv.201600148

Araújo, M. B., Pearson, R. G., Thuiller, W., and Erhard, M. (2005). Validation of species-climate impact models under climate change. *Glob Chang Biol.* 11, 1504–1513. doi: 10.1111/j.1365-2486.2005.01000.x

Auld, B. (1993). Emergence and flowering in *Xanthium spinosum*. *Agric. Ecosyst. Environ*. 47, 215–222. doi: 10.1016/0167-8809(93)90123-7

Auld, B. A., McRae, C. F., and Say, M. M. (1988). Possible control of *Xanthium spinosum* by a fungus. Agriculture, ecosystems and environment. *Agric Ecosyst Environ*. 21, 219–223. doi: 10.1016/0167-8809(88)90089-8

Baldi, S., Bradesi, P., and Muselli, A. (2022). Guaianolide derivatives from the invasive *Xanthium spinosum* L.: evaluation of their allelopathic potential. *Molecules* 27, 7297. doi: 10.3390/molecules27217297

Batterbury, S., and Forsyth, T. (1999). Fighting back: human adaptations in marginal environments. *Environment: Sci. Policy Sustain. Dev.* 41, 6–9. doi: 10.1080/00139159909604639

Beaumont, L. J., Hughes, L., and Pitman, A. J. (2008). Why is the choice of future climate scenarios for species distribution modelling important? *Ecol. Lett.* 11, 1135–1146. doi: 10.1111/j.1461-0248.2008.01231.x

Bellard, C., Bertelsmeier, C., Leadley, P., Thuiller, W., and Courchamp, F. (2012). Impacts of climate change on the future of biodiversity. *Ecol. Lett.* 15, 365–377. doi: 10.1111/j.1461-0248.2011.01736.x

Blackburn, T. M., Pyšek, P., Bacher, S., Carlton, J. T., Duncan, R. P., Jarošík, V., et al. (2011). A proposed unified framework for biological invasions. *Trends Ecol. Evol.* 26, 333–339. doi: 10.1016/j.tree.2011.03.023

Booth, T. H., Nix, H. A., Busby, J. R., and Hutchinson, M. F. (2014). BIOCLIM: the first species distribution modelling package, its early applications and relevance to most current MAXENT studies. *Diversity distributions* 20, 1–9. doi: 10.1111/

Cullen, L. E., and Grierson, P. F. (2007). A sta ble oxygen, but not carbon, isotope chronology of Callitris columellaris reflects recent climate change in north-western Australia. *Climatic Change* 85, 213–229. doi: 10.1007/s10584-006-9206-3

Elith, J., Graham, C. H., Anderson, R. P., Dudík, M., Ferrier, S., Guisan, A., et al. (2006). Novel methods improve prediction of species' distributions from occurrence data. *Ecography* 29, 129–151. doi: 10.1111/j.2006.0906-7590.04596.x

Elith, J., Phillips, S. J., Hastie, T., Dudík, M., Chee, Y. E., and Yates, C. J. (2011). A statistical explanation of MaxEnt for ecologists. *Divers. Distrib* 17, 43–57. doi: 10.1111/j.1472-4642.2010.00725.x

EPPO Global Database (2025). Available online at: https://gd.eppo.int/ (Accessed June 13, 2025).

Evans, J. M., Fletcher, R. J. Jr, and Alavalapati, J. (2010). Using species distribution models to identify suita ble areas for biofuel feedstock production. *Gcb Bioenergy* 2, 63–78. doi: 10.1111/j.1757-1707.2010.01040.x

Gallardo, B., Zieritz, A., and Aldridge, D. C. (2015). The importance of the human footprint in shaping the global distribution of terrestrial, freshwater and marine invaders. *PloS One* 10, e0125801. doi: 10.1371/journal.pone.0125801

Gligor, O., Clichici, S., Moldovan, R., Muntean, D., Vlase, A.-M., Nada, G. C., et al. (2022). Influences of different extraction techniques and their respective parameters on the phytochemical profile and biological activities of *Xanthium spinosum L. extracts. Plants* 12, 96. doi: 10.3390/plants12010096

Goosse, H., Kay, J. E., Armour, K. C., Bodas-Salcedo, A., Chepfer, H., Docquier, D., and Vancoppenolle, M.. (2018). Quantifying climate feedbacks in polar regions. *Nat. Commun.* 9(1), 1919. doi: 10.1038/s41467-018-04173-0

Güez, C. M., Waczuk, E. P., Pereira, K. B., Querol, M. V., Rocha, J. B., and Oliveira, L. F. (2012). *In vivo* and *in vitro* genotoxicity studies of aqueous extract of *Xanthium spinosum*. *Braz. J. Pharm. Sci.* 48, 461–467. doi: 10.1590/s1984-82502012000300013

Guisan, A., and Zimmermann, N. E. (2000). Predictive habitat distribution models in ecology. *Ecol. Modell* 135, 147–186. doi: 10.1016/s0304-3800(00)00354-9

Guo, Y. J., Chen, D., Wang, S. J., Meng, K., and Wang, Y. (2025). Drought legacy influences plant invasion through plant-soil feedback dependent on the origin and lifespan of conditioning species. *Funct. Ecol.* 39, 959–968. doi: 10.1111/1365-2435.70015

Hastie, T., and Tibshirani, R. (1987). Generalized additive models: some applications. J. Am. Stat. Assoc. 82, 371–386. doi: 10.1080/01621459.1987.10478440

Hocking, P. J., and Liddle, M. J. (1986). "The biology of Australian weeds," in *Xanthium occidentale Bertol. complex and Xanthium spinosum L*, 15. (Sydney, Australia: 8th Australian Weeds Conference). doi: 10.5555/19870705692

Hosseini, N., Ghorbanpour, M., and Mostafavi, H. (2024). The influence of climate change on the future distribution of two Thymus species in Iran: MaxEnt model-based prediction. *BMC Plant Biol.* 24, 269. doi: 10.1186/s12870-024-04965-1

Karimmojeni, H., Rahimian, H., Alizadeh, H., Yousefi, A. R., Gonzalez-Andujar, J. L., Sweeney, E. M., et al. (2021). Competitive ability effects of Datura stramonium L. and *Xanthium strumarium* L. on the development of maize (Zea mays) seeds. *Plants* 10, 1922. doi: 10.3390/plants10091922

Ke, C., He, S., and Qin, Y. (2023). Comparison of natural breaks method and frequency ratio dividing attribute intervals for landslide susceptibility mapping. *Bull. Eng. Geol Environ.* 82, 384. doi: 10.1007/s10064-023-03392-0

Kelečević, B., Kovačević, Z., Mitrić, S., and Vrbničanin, S. (2024). Responses of seed germination of *Xanthium orientale* L. and *Xanthium spinosum* L. @ to temperature. *Plant Prot Sci.* 60, 295–304. doi: 10.17221/124/2023-pps

Khadka, D., Babel, M. S., Abatan, A. A., and Collins, M. (2022). An evaluation of CMIP5 and CMIP6 climate models in simulating summer rainfall in the Southeast Asian monsoon domain. *Int. J. Climatol* 42, 1181–1202. doi: 10.1002/joc.7296

Li, G., Huang, J., Guo, H., and Du, S. (2020). Projecting species loss and turnover under climate change for 111 Chinese tree species. *For Ecol. Manage* 477, 118488. doi: 10.1016/j.foreco.2020.118488

Li, J., and Ma, M. (2019). Seeds over-wintering characteristics of Italian Cocklebur and Stab Cocklebur: two invasive plants in Xinjiang, China. S Afr J. Bot. 121, 216–218. doi: 10.1016/j.sajb.2018.10.032

Lin, B., Zhao, Y., Han, P., Yue, W., Ma, X.-Q., Rahman, K., et al. (2014). Antiarthritic activity of *Xanthium strumarium* L. extract on complete Freunds adjuvant induced arthritis in rats. *J. Ethnopharmacol* 155, 248–255. doi: 10.1016/j.jep.2014.05.023

Liu, L., Guan, L., Zhao, H., Huang, Y., Mou, Q., Liu, K., et al. (2021). Modeling habitat suitability of *Houttuynia cordata* Thunb (Ceercao) using MaxEnt under climate change in China. *Ecol. Inform* 63, 101324. doi: 10.1016/j.ecoinf.2021.101324

Liu, Y., Li, Y., Wang, R., Guo, L., Ji, Y., Chen, Y., et al. (2025). Impacts of human activity and climate change on the suita ble habitats for *Xanthium spinosum* in China. *Plants* 14, 306. doi: 10.3390/plants14030306

Löve, D., and Dansereau, P. (1959). Biosystematic studies on *Xanthium*: taxonomic appraisal and ecological status. *Can. J. Bot.* 37, 173–208. doi: 10.1139/b59-016

Martin, R., and Carnahan, J. (1983). The effect of field storage and laboratory conditions on germination of five *Xanthium* species. *Aust. J. Agric. Res.* 34, 249. doi: 10.1071/ar9830249

Marzloff, M. P., Oliver, E. C. J., Barrett, N. S., Holbrook, N. J., James, L., Wotherspoon, S. J., et al. (2018). Differential vulnerability to climate change yields novel deep-reef communities. *Nat. Clim Change* 8, 873–878. doi: 10.1038/s41558-018-0278-7

Máximo, P., Ferreira, L. M., Branco, P. S., and Lourenço, A. (2020). Invasive plants: turning enemies into value. *Molecules* 25, 3529. doi: 10.3390/molecules25153529

Merow, C., MJ, S., TC, E., Guisan, A., SM, M., Normand, S., et al. (2014). What do we gain from simplicity versus complexity in species distribution models? *Ecography* 37, 1267–1281. doi: 10.1111/ecog.00845

Merow, C., Smith, M. J., and Silander, J. A. Jr. (2013). A practical guide to MaxEnt for modeling species' distributions: what it does, and why inputs and settings matter. *Ecography* 36, 1058–1069. doi: 10.1111/j.1600-0587.2013.07872.x

Moore, T. E., Jones, C. S., Chong, C., and Schlichting, C. D.. (2020). Impact of rainfall seasonality on intraspecific trait variation in a shrub from a Mediterranean climate. *Funct. Ecol.* 34(4), 865–876. doi: 10.1111/1365-2435.13533

Muscarella, R., Galante, P. J., Soley-Guardia, M., Boria, R. A., Kass, J. M., Uriarte, M., et al. (2014). ENMeval: an R package for conducting spatially independent evaluations and estimating optimal model complexity for Maxent ecological niche models. *Methods Ecol. Evol.* 5, 1198–1205. doi: 10.1111/2041-210x.12261

Nelder, J. A., and Wedderburn, R. W. M. (1972). Generalized linear models. J. R Stat. Soc. A 135, 370. doi: 10.2307/2344614

Ni, M., and Vellend, M. (2024). Soil properties constrain predicted poleward migration of plants under climate change. *New Phytol.* 241, 131–141. doi: 10.1111/nph.19164

Nooni, I. K., Hagan, D. F. T., Ullah, W., Lu, J., Li, S., Prempeh, N. A., et al. (2022). Projections of Drought characteristics based on the CNRM-CM6 Model over Africa. *Agriculture* 12, 495. doi: 10.3390/agriculture12040495

Pacifici, M., Visconti, P., Butchart, S. H., Watson, J. E., Cassola, F. M., and Rondinini, C. (2017). Species' traits influenced their response to recent climate change. *Nat. Climate Change* 7, 205–208. doi: 10.1038/nclimate3223

Phillips, S. J., Anderson, R. P., Dudík, M., Schapire, R. E., and Blair, M. E. (2017). Opening the black box: an open-source release of Maxent. *Ecography* 40, 887–893. doi: 10.1111/ecog.03049

Phillips, S. J., Anderson, R. P., and Schapire, R. E. (2006). Maximum entropy modeling of species geographic distributions. *Ecol. Modell* 190, 231–259. doi: 10.1016/j.ecolmodel.2005.03.026

- Popp, A., Calvin, K., Fujimori, S., Havlik, P., Humpenöder, F., Stehfest, E., et al. (2017). Land-use futures in the shared socio-economic pathways. *Glob Environ. Change* 42, 331–345. doi: 10.1016/j.gloenvcha.2016.10.002
- Ren, G., Yang, B., Cui, M., Dai, Z., Xiang, Y., Zhang, H., et al. (2022). Warming and elevated nitrogen deposition accelerate the invasion process of Solidago canadensis L. *Ecol. Process* 11, 62. doi: 10.1186/s13717-022-00407-8
- Rupp, D. E., Hawkins, L. R., Li, S., Koszuta, M., and Siler, N. (2022). Spatial patterns of extreme precipitation and their changes under -2 °C global warming: a large-ensemble study of the western USA. *Clim Dyn* 59, 2363–2379. doi: 10.1007/s00382-022-06214-3
- Saeed, A., Hussain, A., Khan, M. I., Arif, M., Maqbool, M. M., Mehmood, H., et al. (2020). The influence of environmental factors on seed germination of *Xanthium strumarium L.*: implications for management. *PloS One* 15, e0241601. doi: 10.1371/journal.pone.0241601
- Santana, P. A., Kumar, L., Da Silva, R. S., Pereira, J. L., Picanço, M. C., et al. (2019). Assessing the impact of climate change on the worldwide distribution of *Dalbulus maidis* (DeLong) using MaxEnt. *Pest Manage*. *Sci.* 75, 2706–2715. doi: 10.1002/ps.5379
- Seebens, H., Blackburn, T. M., Dyer, E. E., Genovesi, P., Hulme, P. E., Jeschke, J. M., et al. (2017). No saturation in the accumulation of alien species worldwide. *Nat. Commun.* 8, 14435. doi: 10.1038/ncomms14435
- Sharma, S., Arunachalam, K., Bhavsar, D., and Kala, R. (2018). Modeling habitat suitability of Perilla frutescens with MaxEnt in Uttarakhand—A conservation approach. *J. Appl. Res. Med. Aromat Plants* 10, 99–105. doi: 10.1016/j.jarmap.2018.02.003
- Stockwell, D. (1999). The GARP modelling system: problems and solutions to automated spatial prediction. *Int. J. Geogr. Inf Sci.* 13, 143–158. doi: 10.1080/136588199241391
- Tang, Y., Luo, M., Wu, S., and Li, X. (2025). Increasing synchrony of extreme heat and precipitation events under climate warming. *Geophys Res. Lett.* 52, e2024GL113021. doi: 10.1029/2024gl113021
- Tao, Y., Shang, T., Yan, J., Hu, Y., Zhao, Y., and Liu, Y. (2022). Effects of sand burial depth on *Xanthium spinosum* seed germination and seedling growth. *BMC Plant Biol.* 22, 43. doi: 10.1186/s12870-022-03424-z
- Teleubay, Z., Yermekov, F., Tokbergenov, I., Toleubekova, Z., Assylkhanova, A., Balgabayev, N., et al. (2023). Identification of potential farm pond sites for spring surface runoff harvesting using an integrated analytical hierarchy process in a GIS environment in Northern Kazakhstan. *Water* 15, 2258. doi: 10.3390/w15122258
- Teng, S. N., Xu, C., Sandel, B., and Svenning, J. (2018). Effects of intrinsic sources of spatial autocorrelation on spatial regression modelling. *Methods Ecol. Evol.* 9, 363–372. doi: 10.1111/2041-210x.12866
- Travis, J. M. J., Delgado, M., Bocedi, G., Baguette, M., Bartoń, K., Bonte, D., et al. (2013). Dispersal and species' responses to climate change. *Oikos* 122, 1532–1540. doi: 10.1111/j.1600-0706.2013.00399.x

Ulrich, W., Soliveres, S., Maestre, F. T., Gotelli, N. J., Quero, J. L., Delgado-Baquerizo, M., et al. (2014). Climate and soil attributes determine plant species turnover in global drylands. *J. biogeography* 41, 2307–2319. doi: 10.1111/jbi.12377

- Van Kleunen, M., Dawson, W., Essl, F., Pergl, J., Winter, M., Weber, E., et al. (2015). Global exchange and accumulation of non-native plants. *Nature* 525, 100–103. doi: 10.1038/nature14910
- Wang, Y., Bu, H., Gu, X., Liu, W., and Wang, X. (2025). Integrated omic analysis provides insights into how Cuscuta australis inhibits the growth and reproduction of *Xanthium spinosum. BMC Plant Biol.* 25, 657. doi: 10.1186/s12870-025-06698-1
- Wan, J. Z., Wang, C. J., and Yu, F. H.. (2019). Effects of occurrence record number, environmental variable number, and spatial scales on MaxEnt distribution modelling for invasive plants. *Biologia* 74, 757–766. doi: 10.2478/s11756-019-00215-0
- Wang, G., and Gou, Q. (2019). Effects of small rainfall events on Haloxylon ammodendron seedling establishment in Northwest China. *Curr. Sci.* 116.1, 121–127. doi: 10.18520/cs/v116/i1/121-127
- Warren, D. L., Matzke, N. J., Cardillo, M., Baumgartner, J. B., Beaumont, L. J., Turelli, M., et al. (2021). ENMTools 1.0: an R package for comparative ecological biogeography. *Ecography* 44, 504–511. doi: 10.1111/ecog.05485
- Watterson, I. G., Chu, Z. W., and Hope, P. K. (2016). Extreme monthly rainfall over Australia in a changing climate. *J. South. Hemisphere Earth Syst. Sci.* 66, 402–423. doi: 10.1071/es16025
- Weber, E. (2017). Invasive plant species of the world: a reference guide to environmental weeds (Wallingford, Oxfordshire: Cabi).
- West, A. M., Kumar, S., Brown, C. S., Stohlgren, T. J., and Bromberg, J. (2016). Field validation of an invasive species Maxent model. *Ecol. Inform* 36, 126–134. doi: 10.1016/j.ecoinf.2016.11.001
- Wiens, J. A., Stralberg, D., Jongsomjit, D., Howell, C. A., and Snyder, M. A. (2009). Niches, models, and climate change: assessing the assumptions and uncertainties. *Proc. Natl. Acad. Sci. U.S.A.* 106, 19729–19736. doi: 10.1073/pnas.0901639106
- Xiao, Y., He, J., Aishan, T., Sui, X., Zhou, Y., and Yimingniyazi, A. (2023). Effects of different degrees of *Xanthium spinosum* invasion on the invasibility of plant communities in the Yili Grassland of Northwest China. *Biology* 13, 14. doi: 10.3390/biology13010014
- Yuan, Z., Zheng, X., Zhao, Y., Liu, Y., Zhou, S., Wei, C., et al. (2018). Phytotoxic compounds isolated from leaves of the invasive weed *Xanthium spinosum*. *Molecules* 23, 2840. doi: 10.3390/molecules23112840
- Zhang, X., Fan, Y., Niu, F., Lu, S., Du, W., Wang, X., et al. (2025). Impacts of climate change on the potential sui table ecological niches of the endemic and endangered conifer *Pinus bungeana* in China. *Forests* 16, 462. doi: 10.3390/f16030462
- Zhang, K., Yao, L., Meng, J., and Tao, J. (2018). Maxent modeling for predicting the potential geographical distribution of two peony species under climate change. *Sci. Total Environ.* 634, 1326–1334. doi: 10.1016/j.scitotenv.2018.04.112
- Zheng, J., and Li, C. (2025). Plant functional diversity as an important mediator of invasive effects on productivity in riparian grasslands. *Biol. Invasions* 27, 1-17. doi: 10.1007/s10530-025-03586-5